Cell Reports, Volume *21*

Supplemental Information

L-Type Voltage-Gated Ca^{2+} Channels Regulate Synaptic Activity-Triggered Recycling Endosome Fusion in Neuronal Dendrites

Brian G. Hiester, Ashley M. Bourke, Brooke L. Sinnen, Sarah G. Cook, Emily S. Gibson, Katharine R. Smith, and Matthew J. Kennedy

Supplemental Experimental Procedures

Expression Constructs

Neurons were transfected using Lipofectamine 2000 (Invitrogen) according to the manufacturer's recommendations and allowed to express plasmids for 48-96 hours prior to experiments. For all assays examining RE fusion, neurons were transfected with a plasmid encoding TfR-mCh-SEP (Kennedy et al., 2010). For experiments examining the RE localization of exogenously expressed GluA1, neurons were transfected with a plasmid encoding SEP-GluA1, which consists of GluA1 N-terminally tagged with Superecliptic pHluorin (SEP) (Wang et al., 2008; Kennedy et al, 2010). For all Ca^{2+} imaging experiments, neurons were transfected with a plasmid encoding the genetically encoded Ca^{2+} indicator GCaMP6s (Chen et al., 2013) (Addgene plasmid #40753) and a plasmid encoding soluble mCh which was used to outline neuron morphology. For Rab11 co-localization experiments, neurons were transfected with a plasmid encoding TfR-mCh and a plasmid encoding GFP-Rab11a (Addgene plasmid #56444). For glutamate antibody internalization experiments neurons were transfected with TfR-mCh to mark REs and a plasmid encoding soluble GFP. For SIM imaging, neurons were transfected with a plasmid encoding soluble mCh to outline neuron morphology and a plasmid encoding TfR fused with a HALO-tag (Grimm et al., 2015) to identify REs.

Pharmacological reagents

DL-AP5 (Tocris, 50-100 µM) and MK801 (Tocris, 10 µM) were used to inhibit NMDA receptors. TTX (Tocris, 1-2 µM) was used to inhibit voltage-gated sodium channels. Nimodipine (Tocris, 1-25 µM), verapamil (Sigma, 25 µM) and diltiazem (Tocris, 50 µM) were used to inhibit L-VGCCs. Bay K8644 (Tocris, 10 µM) was used to agonize L-VGCCs. BAPTA-AM (Invitrogen, 50 µM) was used to chelate intracellular Ca^{2+}.

Glutamate Receptor Internalization Assay

For live-cell antibody feeding experiments, hippocampal neurons transfected with GFP and TfR-mCh were incubated for 1 hr (Fig. 1A, B) at 37°C with 5 µg/mL affinity-purified anti-GluA1 antibody directed against

the extracellular N-terminal domain (Kennedy et al., 2010), or for 3-5 hr at 37°C with either the same affinity-purified anti-GluA1 antibody or 5 µg/mL an anti-GluA2 antibody (MAB397 clone 6C4, EMD Millipore) (Fig. S1A-D). Cells were washed with PBS and fixed for 20 min at room temperature with 4% paraformaldehyde. Cells were blocked overnight with 0.5 mg/mL anti-rabbit F_{ab} (Jackson Immunologicals) in PBS. Cells were post-fixed with 4% paraformaldehyde for 5 min, washed with PBS and permeabilized with 0.1% Triton X-100, then labeled with Alexa 647-conjugated anti-rabbit secondary for 1 hr. Nonpermeabilized cells served as a control to ensure complete blocking of surface bound anti-GluA1 or anti-GluA2, and also served as a quantitative threshold for further analysis. To confirm that internalized signal was not a result of non-specific fluid-phase uptake of anti-GluA1, we performed separate experiments in which we preincubated anti-GluA1 with a 10-fold molar excess of the peptide antigen used to generate the antibody, which eliminated the internal anti-GluA1 signal (Fig. S1E). To quantify the percentage of REs that contain internalized anti-GluA1 or anti-GluA2 antibody, the background-subtracted Alexa 647 fluorescence signal was measured within ROIs drawn over REs in both dendritic spines and dendritic shafts as indicated by the TfR-mCh signal. An identical analysis was performed for both permeabilized and non-permeabilized cells from each antibody feeding assay. To determine whether REs from permeabilized cells were considered AMPA receptor positive, we established a threshold based on the mean signal quantified from RE-based ROIs from control nonpermeabilized cells. Briefly, if the internalized antibody signal (Alexa 647) within REs from permeabilized cells was greater than two standard deviations from the mean signal within REs from nonpermeabilized control cells then we considered those REs as AMPA receptor positive.

To determine the RE-localization of exogenously expressed SEP-GluA1, neurons transfected with TfR-mCh and SEP-GluA1 were imaged in the red (TfR-mCh) and green (SEP-GluA1) channels before and after RE neutralization with ACSF supplemented with 50 mM NH_4Cl (osmolarity adjusted). To quantify the percentage of REs that contained SEP-GluA1, we used a strategy similar to the one described above, with the exception that a given RE was considered SEP-GluA1 positive if the SEP signal within the RE after neutralization was greater than two standard deviations from the mean SEP signal within the RE before neutralization.

Glutamate uncaging

For experiments involving glutamate uncaging, neurons were incubated in an ASCF solution containing (in mM): 130 NaCl, 5 KCl, 10 HEPES, 30 glucose, 0.5 $MgCl_2$, 2 $CaCl_2$, and 0.001 TTX (pH 7.4), supplemented with 2 mM 4-methoxy-7-nitroindolinyl (MNI)-caged L-glutamate (Tocris). Individual dendritic spines were focally stimulated using galvanometric mirrors (FRAPPA, Andor Technologies) to steer a diffraction-limited 405 nm spot. An AOTF was used to gate a 500 µsec pulse of 405 nm light, with the laser intensity adjusted to 5% of total laser power from a 100 mW 405 nm laser that was fiber coupled to the FRAPPA laser-scanning unit. This protocol reliably triggered NMDA receptor-mediated Ca^{2+} transients at individual dendritic spines with similar amplitude and duration as spontaneous NMDA receptor activation by quantal release of glutamate (measured in ACSF lacking Mg^{2+}).

RE fusion stimulation, imaging and analysis

To image RE fusion and cargo delivery, neurons expressing TfR-mCh-SEP were pretreated with 1 µM TTX for 1 hour to inhibit evoked activity. Coverslips with cultured neurons were then placed in a live cell imaging chamber (Ludin) and incubated in baseline ACSF solution containing (in mM): 130 NaCl, 5 KCl, 10 HEPES, 30 glucose, 1 $MgCl_2$, 2 $CaCl_2$, and 0.002 TTX (pH 7.4).

To stimulate synaptic activity (cLTP stimulation), the baseline solution was exchanged for one that contained (in mM): 130 NaCl, 5 KCl, 2 $CaCl_2$, 10 HEPES, 30 glucose, 0 $MgCl_2$, 0 TTX, 0.2 glycine. For minimal stimulation experiments, the baseline solution was exchanged for one that contained (in mM): 130 NaCl, 5 KCl, 2 $CaCl_2$, 10 HEPES, 30 glucose, 0 $MgCl_2$, 0.001 TTX, 0.2 glycine. For KCl-induced membrane depolarization, the baseline solution was exchanged for one that contained (in mM): 85 NaCl, 50 KCl, 2 $CaCl_2$, 10 HEPES, 30 glucose, 1 $MgCl_2$, 0.001 TTX, 0.05 AP5, 0.025 NBQX. For some experimental conditions, this solution was supplemented with AP5 (50 µM).

To locally induce RE fusion by glutamate uncaging, 5-7 sparsely distributed dendritic spines per neuron expressing TfR-mCh-SEP were stimulated by uncaging MNI-glutamate with 30 laser pulses (500 µsec) at a

frequency of 0.5 Hz delivered immediately adjacent to dendritic spines that contained an RE (identified using the mCh signal from TfR-mCh-SEP). To measure the frequency and probability of uncaging-induced RE exocytosis, 2-color (TfR-mCh-SEP) 5 µm z-stacks were acquired every 30 seconds for 5 minutes preceding uncaging, and for 15 minutes following uncaging. Discrete bursts of SEP fluorescence at stimulated dendritic spines that were accompanied by a loss of mCh were classified as RE fusion events.

To measure the delivery of RE cargo to the plasma membrane after stimulation, 1-color (TfR-SEP) 6 µm z-stacks were acquired every 30 seconds before, during and after bath stimulation. Neurons were treated with pharmacolgical antagonists only during stimulation. To quantify the delivery of RE cargo to the PM, a mask was drawn around the imaged portion of the dendritic arbor, and the mean background-subtracted SEP fluorescence signal was quantified in ImageJ. Data are plotted as the ratio of SEP fluorescence at any given time point over the SEP fluorescence at the start of the experiment (SEP F/F_0).

To confirm that the activity-triggered increase in TfR-SEP signal was due to increased surface delivery of RE cargo, we performed three separate experiments. First, to estimate the amount of TfR-SEP signal that is generated from either surface-localized or internal ER-retained TfR-SEP, we used a multi-barrel pipette and a fast stepper motor to switch our normal extracellular ACSF (pH 7.4) to one at pH 6.0 every 2 seconds while imaging a single z-plane of a neuron expressing TfR-SEP at 4Hz (Fig. S2A). Second, to quantify the change in the internal TfR-SEP signal after activity stimulation, we briefly (1 min.) exposed neurons expressing TfR-SEP to ACSF with a pH of 6.0 both before and after cLTP stimulation while imaging as described above (Fig. S2B).Third, to determine the localization of the internal TfR-SEP signal, we imaged live neurons expressing TfR-mCh-SEP before and after exposure to ACSF supplemented with 50 mM NH_4Cl (osmolarity adjusted) to neutralize acidified internal cellular compartments (Fig. S2C).

To measure the rate of RE fusion events in dendritic shafts, a single plane 1-color (TfR-SEP) image was acquired every 250 msec (4 Hz.) for 1 minute in baseline conditions to establish a basal rate of RE fusion, and then again for 2 minutes following cLTP stimulation to measure the activity-induced rate of RE fusion. Neurons were treated with pharmacological antagonists only during activity stimulation. To address the

possibility that the use-dependence of L-VGCC antagonists may lead to incomplete block of channel function, in some experiments neurons were treated with L-VGCC antagonists for 5 min prior to activity stimulation. The results of these experiments were identical to those in which L-VGCC antagonists were added only during activity stimulation. To quantify the rate of shaft RE fusion, discrete bursts of SEP fluorescence within dendritic shafts, indicative of RE fusion events, were counted along the imaged portion of the dendritic arbor for each condition, then plotted as the number of detected RE fusion events per minute.

To measure the rate of RE fusion events in dendritic spines, a 2-color (mCh, SEP) 5 µm z-stack was acquired every 5 seconds for 1 minute prior to and 6 minutes following, bath stimulation. We imaged in this fashion because we found that imaging at a high frame rate in a single z-plane dramatically underestimates the total rate of RE fusion in dendritic spines due to the 3-dimensional nature of neuronal dendrites and spines. To quantify the rate of spine RE fusion, discrete bursts of SEP fluorescence within dendritic spine heads were counted for each neuron and then summed into 1-minute bins. The total number of spine RE fusion events was pooled for all neurons in a given treatment, then plotted as the number of RE fusion events normalized to the first minute of imaging (pre-cLTP stimulation). All RE fusion rate analysis was performed blind to treatment.

To characterize the mode of RE fusion events in dendritic shafts we acquired one color (TfR-SEP) 2.5 µm z-stacks every 500 msec. Each neuron was imaged for two minutes in baseline conditions and for an additional two minutes after cLTP stimulation. For each two-minute imaging session, a small portion of the dendritic arbor was photobleached using the 488 laser (laser intensity 25-40%, 50 µsec pixel dwell time) after 20 imaging frames in order to decrease surface TfR-SEP fluorescence and allow for more sensitive detection of RE fusion events. RE fusion events that occurred within dendritic shafts of this photobleached area were used for further analysis. All subsequent analysis was performed blind to treatment. For each RE fusion event, we measured the SEP signal within a circular ROI that was drawn around the area of the fusion event based on the first frame that the event was detected, then calculated the change in fluorescence over time (F/F_0). If the decline of SEP fluorescence after the fusion event underwent a one-phase

exponential decay to baseline with a $T_{1/2} \leq 5$ sec, then the event was classified as a "burst" event. Otherwise, the event was classified as a "display" event.

To characterize the mode of RE fusion events in dendritic spines, we acquired two color (TfR-mCh-SEP) single plane images every 250 msec for 1 minute in baseline conditions to detect basal spine RE fusion events, and then again for 2 minutes following cLTP stimulation to detect activity-triggered spine RE fusion events. Neurons were treated with pharmacological antagonists only during activity stimulation. To quantify the fraction of spine RE cargo that fused with the membrane and the fraction of spine RE cargo that was delivered to the PM, we utilized a previously published method that takes advantage of the intrinsic SEP/mCh fluorescence ratio of TfR-mCh-SEP at neutral pH (SEP_{neut}/mCh) (Kennedy et al., 2010). We determined SEP_{neut}/mCh for each neuron that we imaged by washing on ACSF supplemented with 50 mM NH_4Cl (osmolarity adjusted) immediately after the imaging period, then measuring and averaging the SEP and mCh signal over several regions of the neuron. We then used this value to normalize the measured SEP and mCh fluorescence signal over time within ROIs drawn over dendritic spines undergoing RE fusion events.

Surface GluA1 quantification

To biochemically quantify activity-dependent changes in total surface GluA1 levels we peformed a surface biotinylation assay as described previously with minor modifications (Sinnen et al., 2016). Briefly, neurons were either exposed to a cLTP stimulation (described previously) or left unstimulated. After cLTP treatment, neurons were washed 3 times in ACSF with 2 mM Ca^{2+}/1 mM Mg^{2+}/1 μM TTX. Neurons were then incubated in ACSF containing 1 mg/ml EZ-link-sulfo-NHS-LC-biotin (Thermo Fisher) for 10 min at room temperature. Neurons were rinsed 3 times in ACSF + 0.1% BSA and then scraped and lysed in 200 μl warm precipitation buffer (PB) containing the following (in mm): 10 $NaPO_4$, pH 7.4, 5 EDTA, 5 EGTA 100 NaCl, 1 Na_3VO_4, 10 sodium pyrophosphate, and 50 NaF with complete ULTRA protease inhibitor mixture tablets (Roche), 1% SDS, and 1% Triton X-100. Lysates were sonicated and centrifuged for 20 min at 18,000 × g. Before pull-down of biotinylated proteins, 10% of the cell lysate was reserved for total input comparison. The remaining sample was combined with NeutrAvidin agarose beads (30 μl; Thermo Fisher)

and incubated overnight at 4°C. The beads were washed 2 times each with PB containing 0.1% Triton X-100, 0.1% Triton X-100 plus 600 mm NaCl, and PB alone. To elute captured proteins, 1× SDS-PAGE buffer was added to the beads and the samples were boiled for 5 min before loading onto 10% SDS-PAGE gels. Immunoblotting was performed with an anti-GluR1 antibody (1:1000, #AB1504; Millipore) and HRP-conjugated secondary antibody (Bio-Rad).

To immunocytochemically quantify activity-dependent changes in total surface GluA1 levels (Fig. S2E, F), neurons were either exposed to a cLTP stimulation (described previously) or left unstimulated. After cLTP treatment, surface GluA1-containing AMPA receptors were labeled by incubating neurons with an antibody directed against the extracellular domain of GluA1 (0.75 μg/mL) diluted in ACSF with 2mM Ca^{2+}/1 mM Mg^{2+} for 15 minutes at 37ºC. Neurons were washed 3 times in ACSF with 2mM Ca^{2+}/1 mM Mg^{2+}, then fixed with 4% paraformaldehyde. After fixation, neurons were permeabilized and then incubated with an antibody directed against the excitatory synapse marker PSD-95 (1:1000, MAB1596, Millipore). Neurons were then washed 3 times with PBS, then labeled with Alexa-561 conjugated anti-mouse secondary (PSD-95) and Alexa-647 conjugated anti-rabbit secondary (GluA1). Fixed and labeled cells were imaged blinded to the treatment using confocal microscopy. Imaging conditions for each channel were determined empirically, then maintained for all cells imaged. Individual dendritic segments were selected for imaging if they met 3 criteria: 1. The dendritic segment emanated from a pyramidal-shaped cell body. 2. The dendritic segment expressed PSD-95. 3. The dendritic segment possessed dendritic spines. For each dendritic segment, a single 5 μm z-stack (0.25 μm step size) was acquired. All image analysis was performed using maximum point-projections created using ImageJ. To measure the amount of surface GluA1, the background-subtracted Alexa 647 signal was measured within a mask drawn over the dendritic segment.

To quantify the amount of newly inserted GluA1-containing AMPA receptors (and not the total surface pool of GluA1-containing AMPA receptors) following stimulation, we first blocked the pre-existing pool of surface GluA1 with an unlabeled primary antibody directed against the extracellular domain of GluA1 (anti-GluA1, 200 μg/mL). Neurons were then stimulated using our previously described cLTP stimulation

for 10 mins. Following stimulation, neurons were incubated with a biotinylated version of the same antibody (anti-GluA1-biotin, 10 μg/mL) for 15 mins in ACSF containing 1 mM Mg^{2+}/2 mM Ca^{2+}. Neurons were washed 3 times in ACSF containing 1 mM Mg^{2+}/2 mM Ca^{2+}/2 μM TTX and fixed with 4% paraformaldehyde. For treatments that included pharmacological inhibitors, the inhibitor was included during the cLTP stimulation, the incubation with the biotinylated antibody and the washes prior to fixation. Neurons were then incubated with Alexa-488 labeled anti-rabbit secondary (1:1000) to label the total pool of surface GluA1 (pre-existing GluA1 plus newly inserted GluA1) and Alexa-647 labeled streptavidin (0.9 μg/mL) to selectively label newly inserted GluA1. Neurons were fixed a second time with 4% paraformaldehyde, washed 3 times with PBS, permeabilized and then incubated with an antibody directed against the excitatory synapse marker PSD-95 (1:1000, MAB1596, Millipore). Neurons were then washed 3 times with PBS and labeled with Alexa-561 conjugated anti-mouse secondary. Fixed and labeled cells were imaged using confocal microscopy. To avoid biasing the selection of dendritic segments during imaging, the signal for the total pool of surface GluA1 (pre-existing GluA1 plus newly inserted GluA1) was used to identify segments for imaging. We used the same criteria as previously described to select dendritic segments. For each dendritic segment, a single 5 μm z-stack (0.25 μm step size) was acquired. All image analysis was performed using maximum point-projections created using ImageJ. To measure the amount of surface GluA1, the background-subtracted Alexa 647 signal was measured within a mask drawn over the dendritic segment defined by the total surface GluA1 signal (Alexa 488).

Ca^{2+} imaging and analysis

To image Ca^{2+} transients during KCl-dependent membrane depolarization, neurons were stimulated as described above. Single z-plane 1-color (GCaMP6s) images of a portion of the dendritic arbor were acquired at a frequency of 4 Hz both before and during stimulation. To quantify the Ca^{2+} signal during KCl stimulation, a mask was drawn around the imaged portion of the dendritic arbor, and the mean background-subtracted GCaMP6s fluorescence signal was measured in ImageJ and plotted as the GCaMP6s $\Delta F/F_0$ over time. Additionally, the measured GCaMP6s signal was summed over a period of 60 seconds starting at stimulation and plotted as the total integrated Ca^{2+} post-KCl stimulation.

To image Ca^{2+} transients during minimal synaptic stimulation, neurons expressing GCaMP6s were stimulated and imaged as described above. To quantify the integrated Ca^{2+} signal within dendritic spines and dendritic shafts during stimulation, ROIs were drawn separately around dendritic spines and dendritic shafts, and the mean background-subtracted GCaMP6s fluorescence signal was measured within those ROIs over the course of two separate 30 second periods, one before and one after stimulation, for control neurons and neurons treated with Bay K8644. These data were then plotted as the ratio of the summed GCaMP6s signal after stimulation over the summed signal before stimulation.

To locally induce Ca^{2+} transients within dendritic spines by glutamate uncaging, approximately 5-7 sparsely distributed dendritic spines per neuron expressing GCaMP6s were stimulated by uncaging MNI-glutamate with 10 laser pulses (500 µsec) delivered immediately adjacent to the surface of the dendritic spine at frequency of 0.5 Hz. To assess the effect of manipulating Ca^{2+} dynamics on glutamate-uncaging induced Ca^{2+} transients, the same dendritic spines were subjected to two separate glutamate uncaging stimulations. The first stimulation served as a baseline measurement, while the second stimulation occurred after neurons were treated with the indicated manipulation, allowing us to make pair-wise comparisons on the same spines. The amplitude of the induced Ca^{2+} transient was quantified in ImageJ by measuring the background-subtracted GCaMP6s fluorescence signal within a circular region of interest (ROI) encompassing the dendritic spine head. The data points in Fig. 2D represent the average fluorescence increase (measured 250 msec after uncaging) of 10 separate uncaging pulses.

TfR and Rab11 co-localization analysis

To determine the extent of co-localization between TfR and Rab11, neurons were transfected with TfR-mCh and GFP-Rab11, then imaged live in an artificial cerebro-spinal fluid (ACSF) containing (in mM): 130 NaCl, 5 KCl, 10 HEPES, 30 glucose, 0.5 $MgCl_2$ and 2 $CaCl_2$ (pH 7.4). For single images comparing the distribution TfR-mCh and GFP-Rab11 in dendrites, we acquired a 2-color 5 µm z-stack. For TfR-mCh and GFP-Rab11 co-migration analysis, we acquired a 2-color single plane image every 250 msec using a dual-bandpass filter (bandpass centered on 512 and 630 nm bandwidth ± 23 nm) and fast AOTF laser switching. We imaged for 20 seconds before, and 60 seconds following, photobleaching both mCh and

GFP fluorescence within a portion of dendrite using the 488 laser (photobleaching laser intensity 40%, 50 µsec pixel dwell time). Photobleaching using the 488 laser was sufficient to bleach both the GFP and mCh signal. We then tracked co-migration of TfR-mCh and GFP-Rab11 positive vesicles into the photobleached area of the dendrite by plotting a kymograph of the TfR-mCh and GFP-Rab11 signal over time for a line drawn along the length of the dendritic segment.

Structured Illumination Microscopy (SIM) and analysis

Multichannel SIM images of neurons expressing mCh and JF646 labeled TfR-HT (Grimm et al., 2015) were acquired with a Nikon N-SIM E structured illumination super-resolution microscope using a 100X 1.49 NA objective, and reconstructed using Nikon Elements software as described previously with minor modifications (Smith et al., 2014). Imaging parameters were determined empirically to produce the best image possible. Acquisition conditions (laser power, exposure time) were adjusted to optimize for a high signal to noise ratio (>8) and to limit exposure time to reduce sample photobleaching (<100 msec). For each coverslip imaged, the objective correction collar was adjusted automatically and a fourier transform (FT) image was used to confirm optimal correction collar adjustment. Z-stacks (z=0.2 µm, 13 slices) were reconstructed using Nikon Elements software. For 3D stack reconstruction, the illumination modulation contrast was set automatically and the high-resolution noise suppression was set to 1, and kept consistent across all images. All SIM image analysis was performed with ImageJ using maximum point z-projection images of each SIM reconstruction. To determine the endosomal content within dendritic spines, the TfR-HT signal for each image was thresholded at 25% above the non-endosomal TfR signal for each neuron. The non-endosomal TfR signal was determined by measuring and averaging the TfR-HT signal at five distinct recycling endosome-negative dendritic spines per neuron. The thresholded TfR-HT signal was then overlayed with the mCh signal for each neuron, and the number of discrete TfR-HT puncta was counted in each discernable dendritic spine. This analysis was peformed blinded to the treatment.

Statistical analysis

Statistical significance for experiments comparing two populations was determined using a two-tailed unpaired Student's *t*-test. In the case that the two populations represented paired measurements, a paired

Student's t-test was used. For experiments comparing three or more populations, a One-way ANOVA with Bonferroni multiple comparison test was used. In cases where measurements were recorded over multiple time points, a one-way repeated measures ANOVA with Bonferroni multiple comparison test was used. For experiments comparing the distribution of two populations, a Kolgomorov-Smirnov test was used. All data are presented as mean ± SEM.

Hiester et al., Figure S1

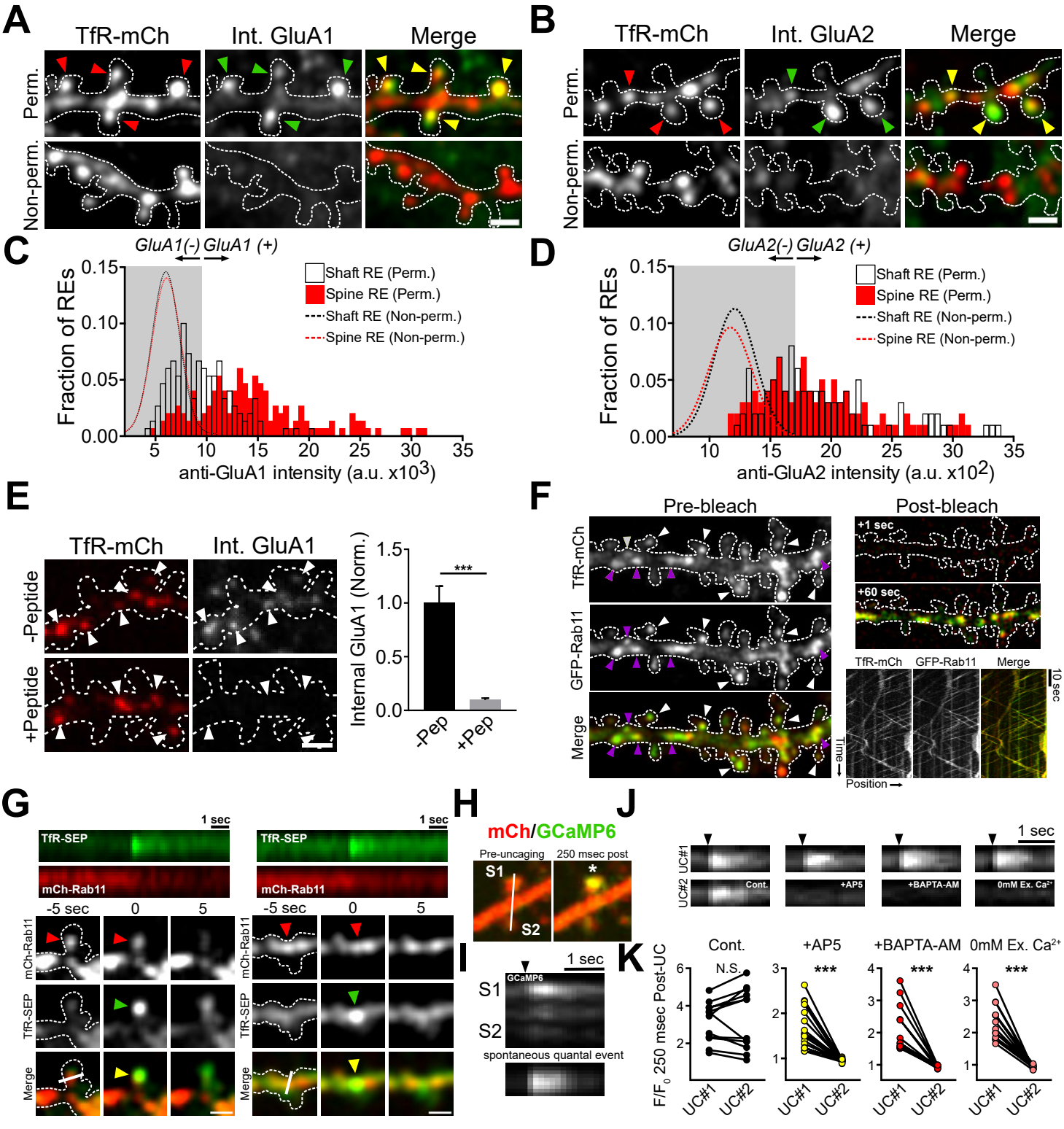

Figure S1. Recycling endosomes harbor AMPA receptors and undergo Ca^{2+}-dependent membrane fusion, Related to Figure 1. (**A** and **B**) Antibody feeding using antibodies directed against AMPA receptor subunits GluA1 (**A**) or GluA2 (**B**). Internalized AMPA receptor antibodies co-localize with TfR-mCh in a large fraction of dendritic spine and shaft REs (arrowheads). Scale bar, 2 µm. (**C** and **D**) Frequency distribution plotting the fraction of REs as a function of the measured intensity of internalized (**C**) GluA1 (permeabilized, n=150 spine REs and 150 shaft REs from 3 neurons; non-permeabilized, n=75 spine REs and 75 shaft REs from 2 neurons) or (**D**) GluA2 (permeabilized, n=100 spine REs and 100 shaft REs from 3 neurons; non-permeabilized, n=60 spine REs and 60 shaft REs from 2 neurons). In each plot, the dotted lines represent the Gaussian fit for non-permeabilized control cells, and the gray box delineates the 2X standard deviation threshold used to determine if an RE contained internalized antibody. (**E**) Pre-incubation of the GluA1 antibody with the peptide used to generate the antibody prevents non-specific uptake. The top panels show the localization of internalized GluA1 antibody (right) within dendritic shaft and spine REs (right) without peptide pre-incubation, while the bottom panel shows the prevention of GluA1 antibody internalization with peptide pre-incubation. Quantification of the total amount of internalized GluA1 antibody with peptide pre-incubation (+Pep, n=10 dendritic segments) normalized to the no-peptide control (-Pep, n=10 dendritic segments) is shown on the right. ***$p<0.001$ (Two-tailed Student's t-test).
(**F**) Tagged TfR constructs co-localized with the RE marker Rab11. Left: Representative maximum projected z-stack of a dendritic segment from a hippocampal neuron expressing TfR-mCh (top panel) and GFP-Rab11 (middle panel) showing co-localization in both dendritic shafts (purple arrowheads) and dendritic spines (white arrowheads). The bottom panel shows the merge of the two channels. Scale bar, 5µm. Right: TfR-mCh (red) and GFP-Rab11 (green) were photobleached to analyze co-trafficking in mobile vesicular pools. Top panels: Single z-plane merged image of the same dendritic segment from (F) 1 sec and 60 sec after photobleaching. Scale bar, 5µm. Bottom panels: Kymograph generated from a line scan drawn along the center of the dendrite shaft for the 60 sec interval following photobleaching showing co-migration of TfR-mCh (left panel) and GFP-Rab11 (middle panel) positive organelles. The right panel shows the merge of the two channels. (**G**) RE fusion in dendritic spines (left) and dendritic shafts (right) are accompanied by a loss of Rab11 signal at the site of RE fusion. For both fusion events, a kymograph of the TfR-SEP and mCh-Rab11 signal generated by the line shown in the bottom left panel is shown on top. The

lower panel shows the mCh-Rab11, TfR-SEP and merged signals during each RE fusion event. Red arrowheads mark the presence of the mCh-Rab11 positive RE while the green and yellow arrowheads indicate the fusion event. Scale bar, 2µm. (**H**) Glutamate uncaging-induced dendritic spine Ca^{2+} transients are driven by NMDA receptor activity. Representative section of dendrite from a hippocampal neuron expressing GCaMP6s and mCh before (left) and 250 msec following (right) uncaging MNI-glutamate near the spine marked with an asterisk. (**I**) Kymograph showing GCaMP6s fluorescence over the line indicated in (H) (top panel). The black arrowhead indicates the time of the uncaging pulse. The bottom panel shows a spontaneous NMDAR-dependent spine Ca^{2+} transient measured in TTX and low Mg^{2+}. (**J**) Representative kymographs of sequential uncaging-induced dendritic spine Ca^{2+} transients at the same spines before (top kymograph) and after (bottom kymograph) application of AP5 (50 µM), BAPTA-AM (50µM, 10 mins) or Ca^{2+} free ACSF (0mM Ex. Ca^{2+} + 1mM EGTA). The black arrowhead indicates the time of the uncaging pulse. (**K**) Quantification of uncaging-induced Ca^{2+} transients before and after treatment. (n=number of spines, Cont. n=12, AP5 n=17, BAPTA-AM n=14, 0mM Ex. Ca^{2+} n=14, ***$p<0.001$, paired t-test).

Hiester et al., Figure S2

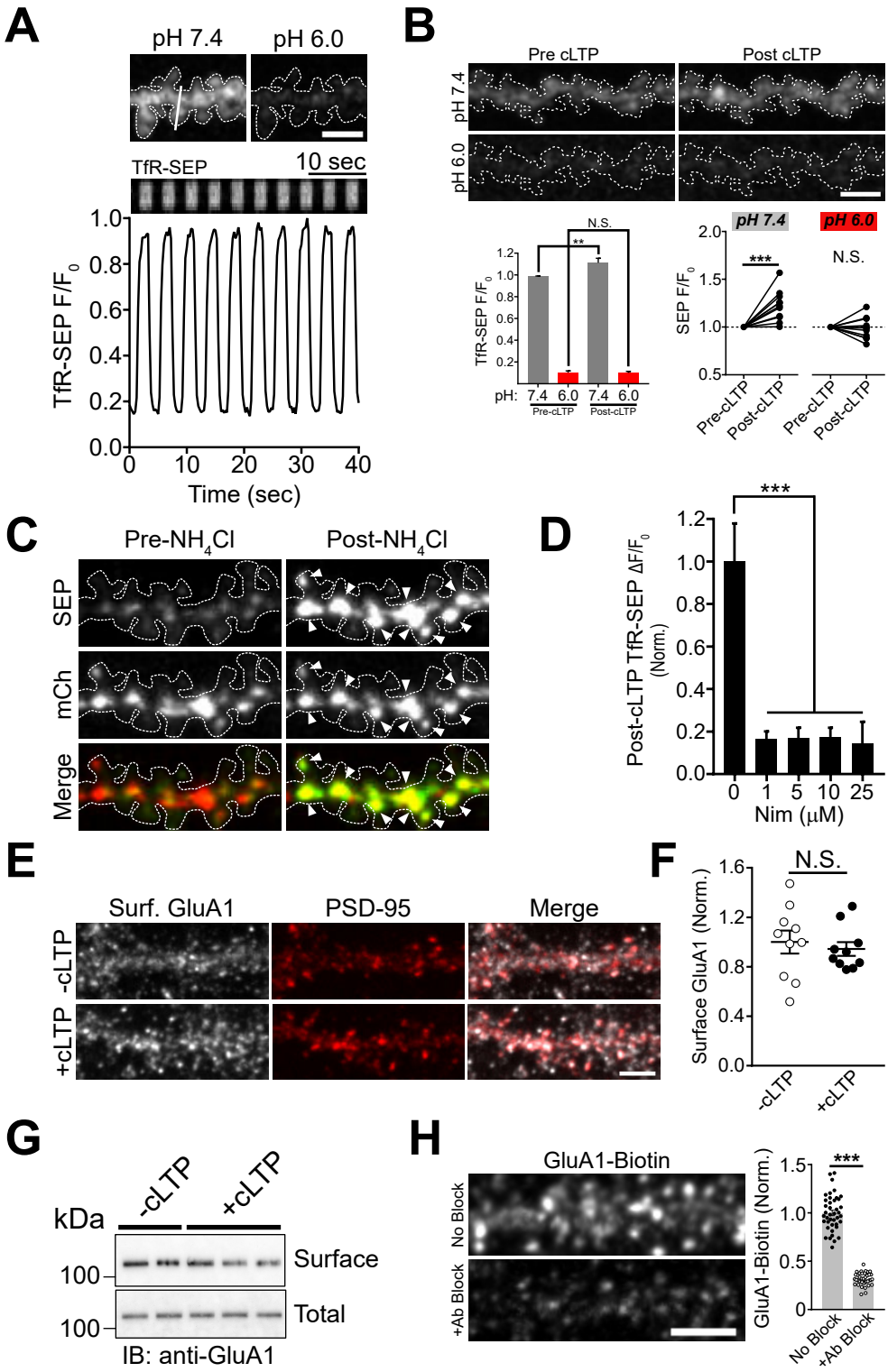

Figure S2. Neural activity promotes delivery of RE cargo and GluA1-containing AMPA receptors to the PM, Related to Figure 2. (**A**) Exposure of TfR-SEP expressing neurons to pH 6.0 rapidly decreases TfR-SEP signal. Top panels: Image of the TfR-SEP signal at pH 7.4 (left) and 2 sec later at pH 6.0 (right). Middle panel: Kymograph of the line indicated above showing the sequential quenching and unquenching of TfR-SEP fluorescence produced by rapidly switching extracellular pH from pH 7.4 to 6.0. Single z-plane images were acquired at 4Hz. Bottom panel: plot showing the quantification of TfR-SEP signal (normalized to the maximum signal) from the kymograph shown above. (**B**) Activity-dependent increase in TfR-SEP signal is not caused by changes in intracellular SEP fluorescence. Images showing the SEP-fluorescence from a representative dendritic segment of a neuron expressing TfR-mCh-SEP at extracellular pH 7.4 (top panels) and pH 6.0 (bottom panels). The left panels show the segment before cLTP stimulation, while the right panels show the same segment after cLTP stimulation. Bottom left: Quantification of the average TfR-SEP signal at pH 7.4 (gray bars) and pH 6.0 (red bars), before and after cLTP stimulation (n=11 neurons). ***p<0.001, N.S.=not significant (One-way ANOVA, Bonferroni multiple comparisons test). Bottom right: Pair-wise comparison of the TfR-SEP signal before and after cLTP stimulation, at pH 7.4 and pH 6.0, normalized to the TfR-SEP signal at baseline for each neuron. ***p<0.001, N.S=not significant (Paired t-test). (**C**) Representative segment of a neuron expressing TfR-mCh-SEP showing the SEP signal (top panels), mCh signal (middle panels) and merged channels (bottom panels), before and after neutralization of internally acidified compartments with 50 mM NH_4Cl. (**D**) Activity-triggered surface delivery of TfR-SEP is inhibited by a range of concentrations of nimodipine. Shown is the quantification of the post-cLTP increase in TfR-SEP signal (normalized to control) for neurons treated with 0, 1, 5, 10 and 25 μM nimodipine during stimulation. ***p<0.001 (One-way ANOVA, Bonferroni multiple comparisons test). (**E-G**) Quantifying the total pool of surface GluA1-containing AMPA receptors after cLTP stimulation. (**E**) Representative dendritic segments of unstimulated (top panels) and cLTP-stimulated (bottom panels) neurons showing the total surface GluA1 signal (left), PSD-95 signal (middle) and merged channels (right). (**F**) Quantification of the total surface GluA1 signal (normalized to unstimulated control) for unstimulated (-cLTP) and cLTP treated (+cLTP) neurons. n=10 neurons per treatment. N.S.=not significant (Two-tailed Student's t-test). (**G**) Western blot of biotinylated surface GluA1 (top) and total GluA1 (bottom) for unstimulated (-cLTP) and cLTP-treated (+cLTP) neurons. (**H**) Incubation with an anti-

GluA1 antibody binds to pre-existing surface GluA1-containing AMPA receptors. The top panel shows the staining for the total amount of surface GluA1 without pre-application of the anti-GluA1 antibody while the bottom panel shows the residual amount of unbound surface GluA1 after anti-GluA1 antibody pre-application. The quantification is shown on the right. (n=number of dendritic segments, No Block n=41, +Block n=39). ***$p<0.001$ (Two-tailed Student's t-test).

Hiester et al., Figure S3

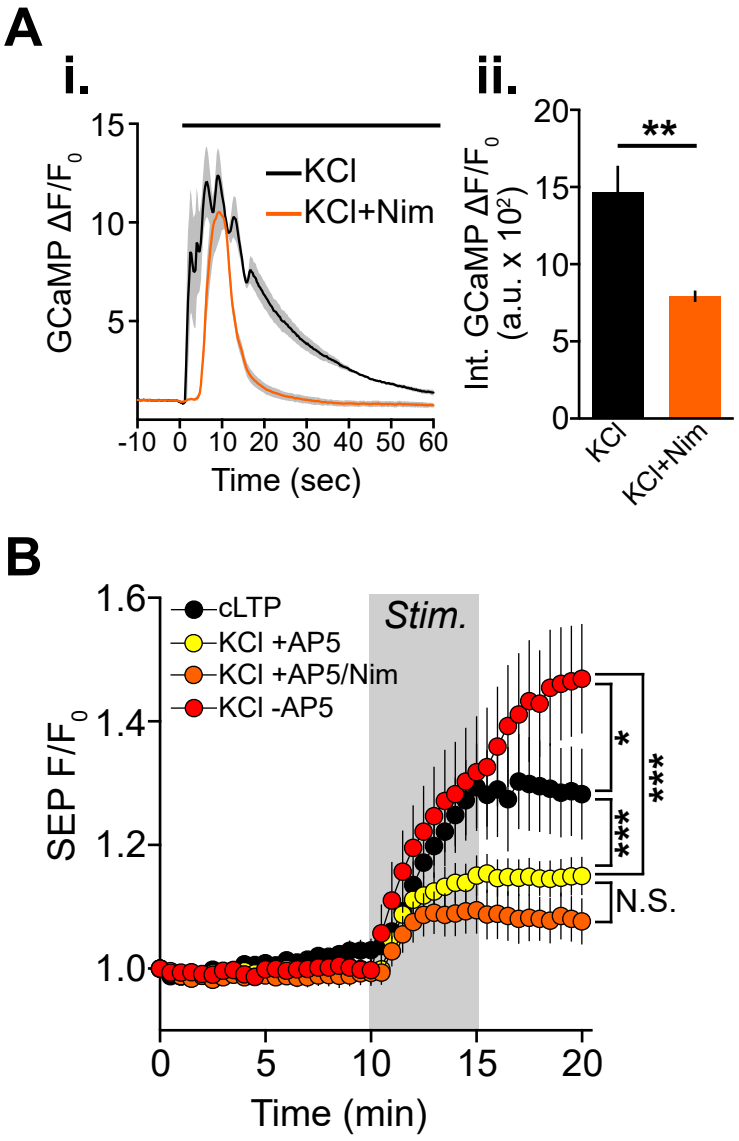

Figure S3. L-VGCC activation alone is not sufficient to trigger robust RE fusion, Related to Figure 3. (**A**) **i.** Ca^{2+} influx over time in response to KCl depolarization measured using GCaMP6s for control and nimodipine treated neurons. Black bar indicates the duration of the KCl stimulus (n=4 neurons per treatment). **ii.** Comparison of the total integrated Ca^{2+} signal post-KCl stimulation for control and nimodipine treated neurons. **p<0.01 (Two-tailed Student's t-test). (**B**) Quantification of RE cargo delivery comparing cLTP stimulus (n=10 neurons), 50mM KCl +AP5 (n=12 neurons), 50mM KCl +AP5/nimodipine (n=12 neurons) and 50mM KCl (n=11 neurons). Gray box indicates the duration of the stimulus. ***p<0.001, **p<0.01 (One-way repeated measures ANOVA, Bonferroni multiple comparisons test).